The features of oscillation pattern in mismatched finite electric ladder filters

S.B. Karavashkin and O.N. Karavashkina

Special Laboratory for Fundamental Elaboration SELF
187 apt., 38 bldg., Prospect Gagarina, Kharkov 61140, Ukraine
phone: +38 0572 276624; e-mail: sbkarav@altavista.com
Website of Laboratory SELF: http://angelfire.lycos.com/la3/SELFlab
Website of the electronic journal SELF Transactions: http://angelfire.lycos.com/la3/selftrans

February 14, 2002

This paper was published first in the electronic journal of laboratory SELF "SELF Transactions", vol.2, issue 1, pp.35-47. Visiting this journal for free at http://angelfire.lycos.com/la3/selftrans you will find many other subjects of mathematical physics and related themes. Already now we have solved many practically important problems which cannot be even approached properly by conventional methods, and this paper corroborates it. This is the future of circuit theory out of which any development in this area is impossible.

You are welcomed to possess this wealth and contact us for discussions and joint further development.

Abstract

Basing on the original relationship of the Dynamical ElectroMechanical Analogy DEMA and original exact analytical solutions for a lumped mechanical elastic line as an analogue, it is studied, how the load resistance effects on the amplitude-frequency and phase-frequency characteristics of mismatched finite ladder filters. It is shown that in filters of such type the indicated characteristics have a brightly expressed resonance form and essentially transform in the lower and medial domains of the pass band, changing insufficiently in the vicinity of cutoff frequency. It disables the conventional method to determine the total phase delay and the ladder filter transmission coefficient and requires finding the exact analytical solutions by way of the presented method. The obtained calculated regularities well agree with the experimental results for similar-parameters ladder filters. The obtained results can be extended to essentially more complicated ladder-filter circuits.

Keywords: Mathematical physics; Wave physics; Circuit theory; ODE; Electric ladder filters; Mismatched ladder filters; Dynamical electromechanical analogy; Transmission lines; Networks; Elastic lumped lines

Classification by MSC 2000: 30E25; 93A30; 93C05; 94C05

Classification by PASC 2001: 02.60.Li; 84.30.Vn; 84.40.Az

1. Introduction

The basic calculation method for electric ladder filters is the two-port method and those developed on its basis. It is accepted that “one of the two-port method advantages is that the complicated circuit can be reduced to a few two-ports connection. The coefficients of each are easy expressed through the element parameters of the related sections of the circuit. And a few two-ports connection in its turn can be presented as some resulting two-port. The finding of the coefficient matrix is reduced mostly to summing and multiplying the matrixes of the separate two-ports into which the considered circuit is factored” [1, p. 53]. With the obviously simple and effective approach, this method has essential restrictions when applied. Specifically, when calculating ladder filters, it is supposed that the input and output of their sections are matched, as "usually one seeks to insert separate sections of the laddered circuit matched" [2, p. 269]. The more, "the inserted sections must be matched always, as only at this condition one can sum the characteristic constants of the transmission" [3, p. 120]. Just because of it "if the circuit was set up of T-sections, it must begin and finish with the impedance $Z_1/2$, and if of pi-sections – with the parallel impedance $2Z_2$" [4, p. 603]. Considering the filter circuits, one supposes that the filter input and output are matched with the source of e.m.f. and with the load, i.e., that each section of the filter and the circuit on the whole are loaded on the impedance equal to that characteristic. In the reality this condition is not satisfied, as the characteristic impedance of the filter depends on the frequency; it has a real value at the transparency band and is reactive at the stop band" [4, p. 623]. Furthermore, "unfortunately, the characteristic impedances of sections are expressed by the functions physically unrealisable, and by this reason one can proceed the matched connection in real circuits only approximately" [3, p. 120].

This misfit of the two-port method approach to the real processes in ladder filters is caused by the fact that at the mismatched load the influence of the wave properties of the filter as a whole is revealed. For example, in [5] in the case of many-sectioned wave-guides, it is experimentally established that "the lengths of the arbitrarily chosen sections scatter coherently the chopped reflections and make the ripples … The reflected signal amplitude growing in excess of its end-to-end response can be raised by single reflected signals from the points far from the source" [5].

In this paper we will modify the approach to the ladder filters calculation, using the original Dynamical ElectroMechanical Analogy (DEMA) whose foundations have been stated in [6]. The conventional electromechanical analogy has the following known basis: "to each dependent variable and all derivatives of one system (i.e., x, dx/dt, d^2x/dt^2), the variable having similar derivatives (q, dq/dt, d^2q/dt^2) corresponds, and the related functions are interconnected so that if some function of one system is known, the corresponding function of the second system can be found" [7, pp. 88 – 89]. On distinct from this, we will use the known property of the modelling system of equations for ladder filters, which admits to separate the time and spatial variables. And we will compare the mechanical and electrical models as the whole, grounding on the correspondence of the modelling systems of *algebraic* equations obtained from those differential after the time dependence eliminating. It will enable us to be not fixed so rigidly to the correspondence of the circuit particular elements and to be not limited in the range of analogues by differentiating or integrating the modelling differential equations. So, with the new relationship of models, the circuits vibration pattern can basically differ, retaining the correspondence between the models, since the base principles will be more generalised when choosing the analogues. These principles will be connected with the boundary conditions, with the features of mechanical system of an elastic line as a whole, but the main, with the correspondence of the modelling systems of *algebraic* equations. Namely the systems of algebraic equations, not one differential equation of the electrical circuit on whose base the relationship of the analogy was established up to now (see, e.g., [7, p. 89], [8, pp. 32 – 34]), referring to the two-port technique. The possibility to introduce such an analogy was indicated by Atkinson in [9, p. 32 – 33]. However the matrix technique to obtain the solutions for mechanical systems enabled Atkinson neither to develop this direction nor to exceed the frames of simplest LC and CL ladder filters nor to write in general form the relationship between compared systems nor to obtain the solutions in the analytical form.

To avoid the complication appearing when using the matrix techniques, we will use, in addition to DEMA, the exact analytical solutions for mechanical lines presented in [10] and [11]. Their main distinction is that when finding the solutions using the non-matrix technique, we have no need to study the eigenvalues and natural frequencies of a mechanical line as the base to find these solutions. The exact solution is found directly for a specific modelling system of differential equations which accounts all the features defined by the initial and boundary conditions, and the solutions are presented not in the matrix form or as the recurrent relationship but in the analytical form.

Combining these two methods, we have no need to consider a ladder filter as a simple assemblage of specific two-ports. As we will show in this paper, it enables us to extend essentially the calculation scope and to study the exact patterns of processes for the much broader range of models than the conventional two-port method enables.

2. The generalised system DEMA

Before we get down the main purpose of our investigation, let us generalise the relationships of the electromechanical analogy presented in [6]. Realising the approach stated in the introduction to set up the electromechanical analogy between the systems, obtain the relationship of our interest by direct comparison of the modelling systems of the algebraic equations of related models. It will be sufficient to use any two models of the studied kind, for example, a semi-finite mechanical line and the electrical filter corresponding to it. Their general form is shown in Fig. 1.

The modelling system of differential equations for a semi-finite mechanical elastic line, Fig. 1a, has the following form:

$$
\begin{aligned}
& m\frac{d^2\Delta_1}{dt^2} = F(t) + s(\Delta_2 - \Delta_1) \\
& m\frac{d^2\Delta_2}{dt^2} = s(\Delta_3 + \Delta_1 - 2\Delta_2) \\
& \ldots\ldots\ldots\ldots\ldots\ldots\ldots\ldots\ldots\ldots\ldots \\
& m\frac{d^2\Delta_n}{dt^2} = s(\Delta_{n+1} + \Delta_{n-1} - 2\Delta_n) \\
& \ldots\ldots\ldots\ldots\ldots\ldots\ldots\ldots\ldots\ldots\ldots ,
\end{aligned}
\tag{1}
$$

where $F(t) = F_0\, e^{j(\omega t+\varphi_0)}$ is the external acting force; Δ_n is the momentary displacement of the nth mass from the state of rest; s is the line stiffness coefficient; m is the line elements mass; φ_0 is the initial phase of the external excitation; $n = 1, 2, 3, ...$ is the line element number.

To establish the electromechanical analogy, we have to transform (1) to the form convenient for it. Present Δ_n in the form

$$\Delta_n = \delta_n\, e^{j(\omega t+\varphi_0)}, \tag{2}$$

where δ_n is the displacement amplitude of the nth element. We yield

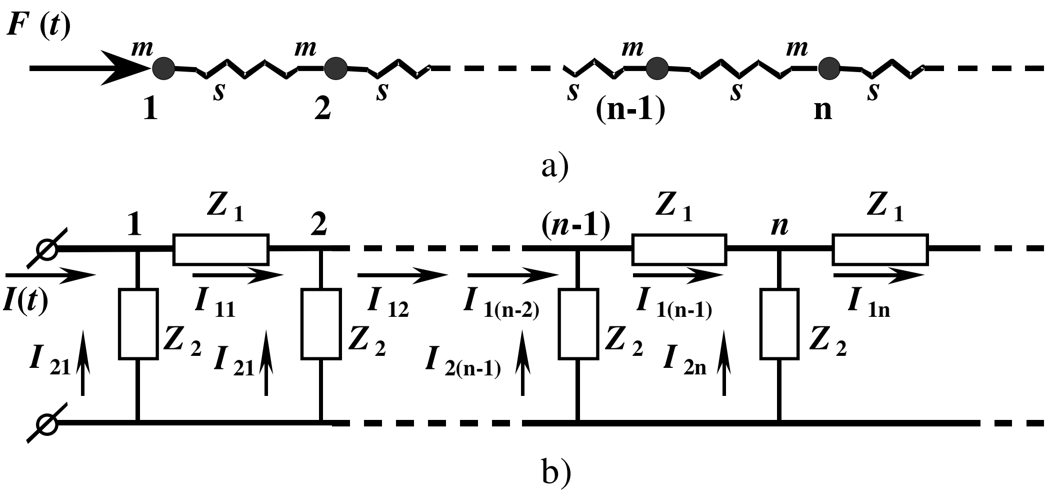

Fig. 1. The schematic diagram of a semi-finite mechanical elastic line (a) and of corresponding ladder filter (b)

$$\begin{aligned}
&-\omega^2 m\delta_1 = F_0 + s\left(\delta_2 - \delta_1\right)\\
&-\omega^2 m\delta_2 = s\left(\delta_3 + \delta_1 - 2\delta_2\right)\\
&\ldots\ldots\ldots\ldots\ldots\ldots\ldots\ldots\ldots\ldots\ldots\\
&-\omega^2 m\delta_n = s\left(\delta_{n+1} + \delta_{n-1} - 2\delta_n\right)\\
&\ldots\ldots\ldots\ldots\ldots\ldots\ldots\ldots\ldots\ldots\ldots\ .
\end{aligned} \tag{3}$$

We will determine the modelling system of differential equations for the ladder filter conventionally, using the first Kirchhoff law for the node indicated in Fig. 1b. Direct the currents in the filter longitudinal elements with the external current, and in the parallel elements – to the selected nodes of the filter. With it the modelling system takes the following form:

$$\begin{aligned}
&\dot I(t) = -\dot I_{21} + \dot I_{11}\\
&\dot I_{11} = -\dot I_{22} + \dot I_{12}\\
&\ldots\ldots\ldots\ldots\ldots\ldots\ldots\ldots\\
&\dot I_{1(n-2)} = -\dot I_{2(n-1)} + \dot I_{1(n-1)}\\
&\dot I_{1(n-1)} = -\dot I_{2n} + \dot I_{1n}\\
&\ldots\ldots\ldots\ldots\ldots\ldots\ldots\ldots\ .
\end{aligned} \tag{4}$$

Using the conventional regularities

$$\dot I_{1n} = \frac{\dot U_{n+1} - \dot U_n}{\dot Z_1}; \qquad \dot I_{2n} = \frac{\dot U_n}{\dot Z_2}, \tag{5}$$

where $\dot U_n$ is the voltage at the nth node with respect to common wire, and presenting

$$\begin{aligned}
&I(t) = i_0\, e^{j(\omega t+\varphi_0)};\ \dot I_{1n} = i_{1n}\, e^{j(\omega t+\varphi_0)};\\
&\dot I_{2n} = i_{2n}\, e^{j(\omega t+\varphi_0)};\ \dot U_n = u_n\, e^{j(\omega t+\varphi_0)},
\end{aligned} \tag{6}$$

we yield the sought modelling system of equations for a semi-finite homogeneous ladder filter:

$$\begin{aligned}
&\frac{1}{\dot Z_2}u_1 = -i_0 + \frac{1}{\dot Z_1}\left(u_2 - u_1\right)\\
&\frac{1}{\dot Z_2}u_2 = \frac{1}{\dot Z_1}\left(u_3 + u_1 - 2u_2\right)\\
&\ldots\ldots\ldots\ldots\ldots\ldots\ldots\ldots\ldots\ldots\ldots\\
&\frac{1}{\dot Z_2}u_{n-1} = \frac{1}{\dot Z_1}\left(u_n + u_{n-2} - 2u_{n-1}\right)\\
&\frac{1}{\dot Z_2}u_n = \frac{1}{\dot Z_1}\left(u_{n+1} + u_{n-1} - 2u_n\right)\\
&\ldots\ldots\ldots\ldots\ldots\ldots\ldots\ldots\ldots\ldots\ldots\ .
\end{aligned} \tag{7}$$

Comparing (3) and (7), we yield the sought relationship between the electrical ladder filter and mechanical long line:

$$\begin{aligned}
&u_n \leftrightarrow \delta_n; \qquad -i_0 \leftrightarrow F_0;\\
&\frac{1}{\dot Z_1} \leftrightarrow s; \qquad \frac{1}{\dot Z_2} \leftrightarrow -\omega^2 m.
\end{aligned} \tag{8}$$

The relationship (8) essentially differs from the conventional system of electromechanical analogy shown in Table 1 [8, p. 32, 34], [12, p. 15], [13, p. 471]. Particularly, in (8) the elements mass and the mechanical line stiffness correspond not to the specific inductance or capacitance but to the longitudinal and transversal conductance of the electrical filter section relatively. Due to it, as an active electrical conductance as some complicated-form complex conductance as the input resistance of some ladder filter being the subsystem of a studied branched filter can correspond to them. While according to Table 1, only the active resistance of a mechanical elastic line can correspond to the active resistance of an electrical circuit. And relatively to the impedances it is also accepted that the change of the capacitive pattern of the analogue to that inductive (and vice versa) must be accompanied by change of the system of analogy (see, e.g., [8, pp. 33 – 34]). In the relationship (8) we need not such operation.

Table 1. Unified system of electromechanical analogies

Electrical value	Mechanical value	
	1^{st} system	2^{nd} system
voltage (e.m.f.) U	force F	velocity v
current i	velocity v	force F
inductance L	mass m	pliability c_m
capacitance C	pliability c_m	mass m
active resistance r	active mechanical resistance r_m	active mechanical conduction $1/r_m$

Furthermore, in the relationship (8) the external excitation frequency is important, because the initial system (1) modelling a mechanical line is the system of the second-order ODE with constant coefficients, while an electrical line is modelled by the integro-differential equations (5). This is why, before establishing the relationship between the models, one had to reduce both systems to a common algebraic form. The dependence on frequency ω appearing in the relationship (8) became the direct consequence of this reduction. And one cannot yield the relationship (8) by the differentiation or integration within the frames of conventional approach. Only transiting from the system of differential equations to the algebraic system, the above feature in the relationship of the electromechanical analogy appears.

The basic difference between the conventional analogy systems in the Table 1 and the system (8) furnishes to say that the ladder filters are inherent in their own system of correspondence which due to its features has been determined as the Dynamical System of ElectroMechanical Analogy (DEMA).

One of its main advantages is that it is based on the complete complex of solutions for a mechanical elastic line, including the solutions for forced and free vibrations. Connecting the different fields of knowledge with the help of DEMA, one can, using the new results in mechanics, first, to provide the development in the field of ladder filters (and with them the cascades, networks, transmission lines etc,); second, to combine the diversiform models, providing the wider scope for the mathematical and physical modelling of the most diversiform by their nature processes and systems. In this way we approach to the most general concept of the analogous models having been formulated by Karplus: “Two systems are analogous if their reactions to the similar excitations reveal in a similar form” [8, p. 36].

3. The unloaded and shorted finite ladder filters

Using the DEMA relationship and results [11], determine the characteristics of an unloaded and shorted ladder filter. In Fig. 2 the diagrams of mechanical elastic line with unfixed end containing n masses are shown as well as an equivalent ladder filter with an open output. On the basis of solutions presented in [11] and relationship (8), the solutions for an unloaded electrical filter will have the following form:

at the pass band, $\beta_{el} < 1$

$$\dot{U}_i = \frac{i_0\sqrt{-\dot{Z}_1\dot{Z}_2}\cos\left[2(n-i)+1\right]\tau_{el}}{\sin 2n\tau_{el}} e^{j(\omega t+\varphi_0)}, \tag{9}$$

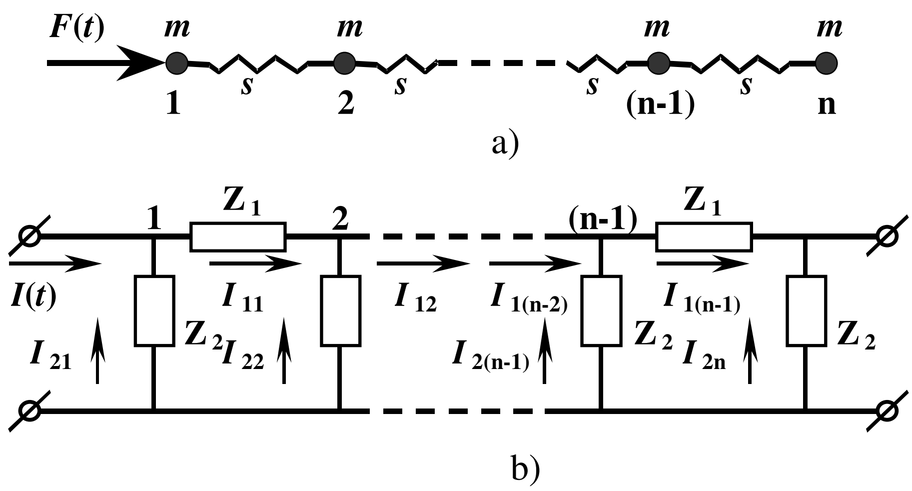

Fig. 2. The schematic diagram of a finite mechanical elastic line with unfixed end (a) and of corresponding ladder filter (b)

at the stop band, $\beta_{el} > 1$

$$\dot{U}_i = (-1)^{i+1} \frac{i_0\sqrt{-\dot{Z}_1\dot{Z}_2}\left[\gamma_{el+}^{2(n-i)+1} - \gamma_{el-}^{2(n-i)+1}\right]}{\left[\gamma_{el+}^{2n} - \gamma_{el-}^{2n}\right]} e^{j(\omega t+\varphi_0)} \tag{10}$$

and at the cutoff frequency, $\beta_{el} = 1$

$$\dot{U}_i = (-1)^{i+1} \frac{i_0\sqrt{-\dot{Z}_1\dot{Z}_2}\left[2(n-i)+1\right]}{4n} e^{j(\omega t+\varphi_0)}, \tag{11}$$

where ω is the external current $I(t)$ frequency, φ is the external current $I(t)$ initial phase, $\beta_{el} = \sqrt{-\dot{Z}_1 / 4\dot{Z}_2}$, $\tau_{el} = \arcsin \beta_{el}$, $\gamma_{el+} = \beta_{el} + \sqrt{\beta_{el}{}^2 - 1}$, $\gamma_{el-} = \beta_{el} - \sqrt{\beta_{el}{}^2 - 1}$, $i = 1, 2, ..., n$ is the number of the studied node of the filter, and n in this case and further is the number of the calculated nodes of the filter.

As conventionally, at the pass band the solutions describe the standing vibrations with n resonances arising at the condition

$$\sin 2n\tau_{el} = 0. \tag{12}$$

The input resistance of the filter for which, in case of the load absence at its end, we will write $\dot{Z}_{oc}$ is equal:

at the pass band, $\beta_{el} < 1$

$$\dot{Z}_{oc} = \frac{\dot{U}_1}{i_0 e^{j(\omega t+\varphi_0)}} = \frac{\sqrt{-\dot{Z}_1\dot{Z}_2}\cos\left[2n-1\right]\tau_{el}}{\sin 2n\tau_{el}}, \tag{13}$$

at the stop band, $\beta_{el} > 1$

$$\dot{Z}_{oc} = \frac{\dot{U}_1}{i_0 e^{j(\omega t+\varphi_0)}} = (-1)^{i+1} \frac{\sqrt{-\dot{Z}_1\dot{Z}_2}\left[\gamma_{el+}^{2n-1} - \gamma_{el-}^{2n-1}\right]}{\left[\gamma_{el+}^{2n} - \gamma_{el-}^{2n}\right]} \tag{14}$$

and at the cutoff frequency, $\beta_{el} = 1$

$$\dot{Z}_{oc} = (-1)^{i+1} \frac{\dot{U}_1}{i_0 e^{j(\omega t+\varphi_0)}} = \frac{\sqrt{-\dot{Z}_1\dot{Z}_2}\left[2n-1\right]}{2n}. \tag{15}$$

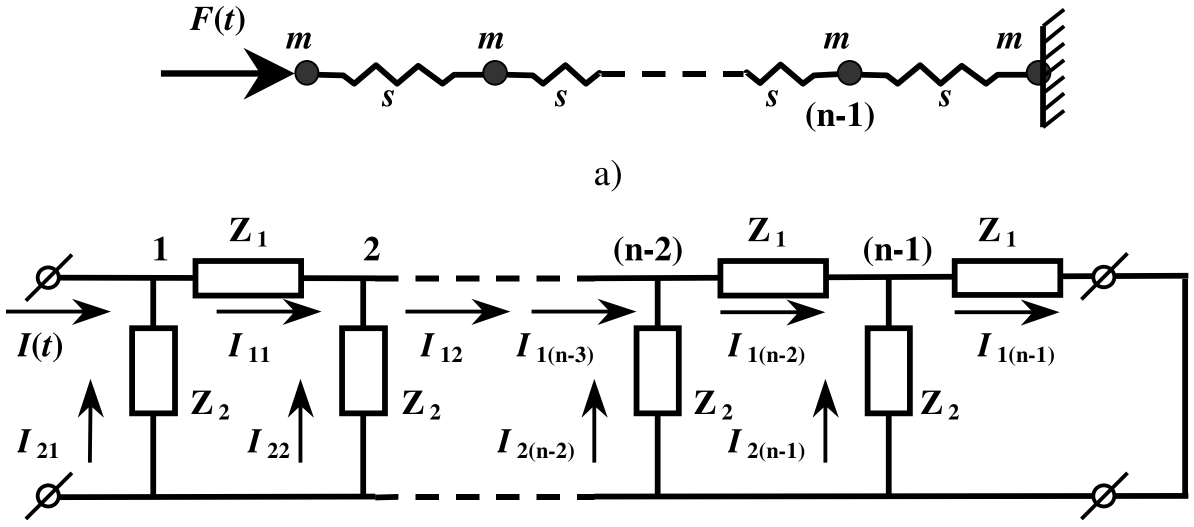

a) b)

Fig. 3. The schematic diagram of a finite mechanical elastic line with fixed end (a) and of corresponding ladder filter with shorted output (b)

At the pass band, dependently on $\dot{Z}_1$ and $\dot{Z}_2$, the resistance R_{oc} can be active, inductive or capacitive. But the main, in any case its amplitude-frequency characteristic will have also n resonances. At the stop band with the frequency growth the input resistance monotonously tends to zero proportionally to $\sim 1/\gamma_{el+}$. And only at the cutoff frequency and at large n the input resistance is approximately equal in its amplitude to the impedance $\sqrt{\dot{Z}_1\dot{Z}_2}$. It essentially differs from the results obtained by the two-port method (see, e.g., [4, p. 606]. One more important feature of the presented solutions is that the vibration amplitude of the last filter section ($i = n$) is not maximal, as we used to think by the analogy with electrical distributed transmission lines. According to (9), it differs by the multiplier $\cos\tau_{el}$ and diminishes to zero with the vibration frequency approaching to that critical (or $\tau_{el} \to \pi/2$, which is tantamountly).

For a ladder filter with the shorted output the situation will be similar. In Fig. 3a we show the model of a finite mechanical line whose nth element is fixed, and in Fig. 3b – the corresponding diagram of an electric ladder filter with the shortened output. Noting [11] and relations (8), we can describe the process in the studied filter by the following system of expressions:
at the pass band of the filter, $\beta_{el} < 1$

$$\dot{U}_i = -\frac{i_0\sqrt{-\dot{Z}_1\dot{Z}_2}\sin 2(n-i)\tau_{el}}{\cos(2n-1)\tau_{el}}e^{j(\omega t+\varphi_0)} \tag{16}$$

at the stop band, $\beta_{el} > 1$

$$\dot{U}_i = (-1)^{i+1}\frac{i_0\sqrt{-\dot{Z}_1\dot{Z}_2}\left[\gamma_{el+}^{2(n-i)} - \gamma_{el-}^{2(n-i)}\right]}{\left[\gamma_{el+}^{2n-1} - \gamma_{el-}^{2n-1}\right]}e^{j(\omega t+\varphi_0)}; \tag{17}$$

and at the cutoff frequency, $\beta_{el} = 1$

$$\dot{U}_i = (-1)^{i+1}\frac{i_0\sqrt{-\dot{Z}_1\dot{Z}_2}\,2(n-i)}{(2n-1)}e^{j(\omega t+\varphi_0)}. \tag{18}$$

The same as in case of unloaded filter, at the transparency band we see n resonance peaks (taking into account the nth shorted node). The conditions of their appearance are determined now by the vanishing denominator of (16). The filter input resistance written as $\dot{Z}_{sc}$ for the filter with the shorted output

also essentially differs from the results obtained by the two-port method. Its value will be determined now by the following system of expressions:
at the pass band of the filter, $\beta_{el} < 1$

$$\dot{Z}_{sc} = \frac{\dot{U}_1}{i_0 e^{j(\omega t+\varphi_0)}} = -\frac{\sqrt{-\dot{Z}_1\dot{Z}_2}\sin 2(n-1)\tau_{el}}{\cos(2n-1)\tau_{el}}, \tag{19}$$

at the stop band, $\beta_{el} > 1$

$$\dot{Z}_{sc} = \frac{\dot{U}_1}{i_0 e^{j(\omega t+\varphi_0)}} = \frac{\sqrt{-\dot{Z}_1\dot{Z}_2}\left[\gamma_{el+}^{2(n-1)} - \gamma_{el-}^{2(n-1)}\right]}{\left[\gamma_{el+}^{2n-1} - \gamma_{el-}^{2n-1}\right]}; \tag{20}$$

and at the cutoff frequency, $\beta_{el} = 1$

$$\dot{Z}_{sc} = \frac{\dot{U}_1}{i_0 e^{j(\omega t+\varphi_0)}} = \frac{\sqrt{-\dot{Z}_1\dot{Z}_2}\,2(n-1)}{(2n-1)}. \tag{21}$$

We see from (19) – (21) that at the pass band the input resistance will have $(n-1)$ resonance peaks. At the stop band the resistance falls with frequency proportionally to $1/\gamma_{el+}$, and with the boundary frequency it is equal in amplitude to the impedance only at large n.

As the results have been refined, the relation between the ladder filter natural impedance and the filter input resistance (being important for calculations) will essentially change. We can determine it by an analogy with electrical transmission lines as follows (see, e.g., [4, p. 572]):

$$\dot{Z}_0 = \sqrt{Z_{oc}Z_{sc}}\ . \tag{22}$$

Substituting sequentially (13) – (15) and (19) – (21) into (22), we can see that in general case the conventional equality (22) is not true. It speaks that for ladder filters this method to find the natural impedance is unacceptable. Although for the single filters the conventional computations retain true, the same as the two-port method itself.

The reason of discrepancy of the results obtained with the help of DEMA and by the two-port method is the same. The same as (16) – (18), solutions (9) – (11) describe the standing wave – just the process which has to take place when the load mismatched and in this connection the waves reflected from the

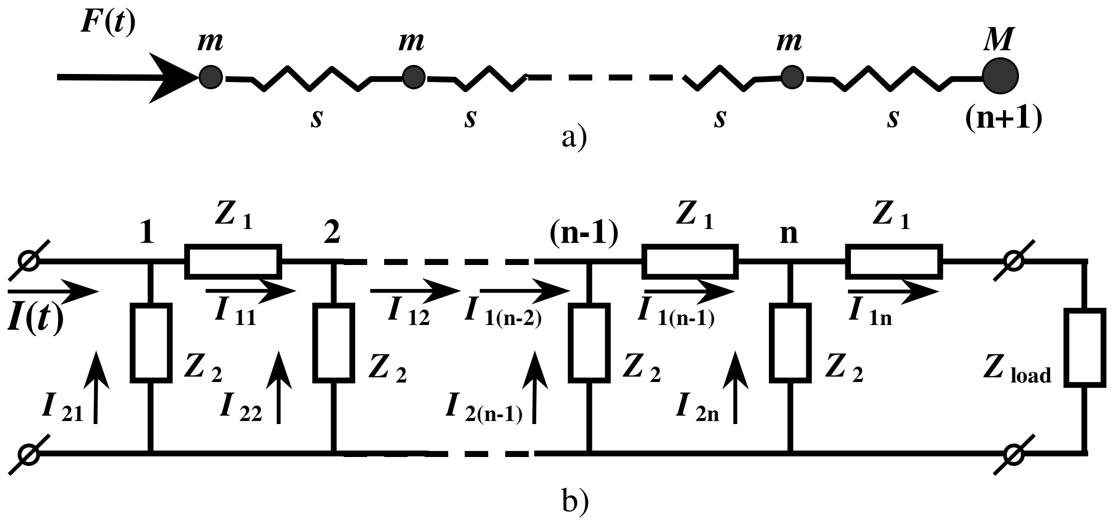

Fig. 4. The schematic diagram of a finite mechanical elastic line with the mass $M \neq m$ at its end (a) and of corresponding ladder filter with the arbitrary load $\dot{Z}_{load}$ (b)

ends of the filter are produced. The two-port method does not take it into account. And in the finite filters we also cannot obtain the solution on the basis of a simple superposition of direct and reverse waves, since in these filters the multiple reflections from both ends take place. So, in general case, we cannot use for sure the idle run and shorting regimes to find the filter natural impedance. We have to determine it on the basis of complete analytical solutions – just so as we did it with the help of DEMA.

4. An arbitrarily loaded finite ladder filter

In ladder filters practical calculations the most important is the case when the filter is loaded arbitrarily. As we saw in the introduction, generally the two-port method cannot solve this problem, because its application requires, the filter output impedance to be matched with the load. The assemblage of the method DEMA with the method to obtain exact analytical solutions for mechanical analogues enables us to find the solutions so necessary for the practice.

Take as the mechanical analogue a finite elastic lumped line shown in Fig. 4a, whose last $(n+1)$th element has the mass M different from the rest of elements. The exact analytical solutions for this model have the following form:

in the periodical vibration regime at $\beta<1$

$$\Delta_i=\frac{F_0e^{j(\omega t+\varphi_0)}\left\{M\omega\sin\left[2(n-i)+2\right]\tau-\sqrt{sm}\cos\left[2(n-i)+1\right]\tau\right\}}{\omega\sqrt{sm}\left\{M\omega\cos\left[2n+1\right]\tau+\sqrt{sm}\sin 2n\tau\right\}} \tag{23}$$

in the aperiodical vibration regime at $\beta>1$

$$\Delta_i=(-1)^i\frac{F_0e^{j(\omega t+\varphi_0)}\left[M\omega\left(\gamma_+^{2(n-i+1)}-\gamma_-^{2(n-i+1)}\right)-\sqrt{sm}\left(\gamma_+^{2(n-i)+1}-\gamma_+^{2(n-i)+1}\right)\right]}{\omega\sqrt{sm}\left[M\omega\left(\gamma_+^{2n+1}-\gamma_-^{2n+1}\right)-\sqrt{sm}\left(\gamma_+^{2n}-\gamma_+^{2n}\right)\right]} \tag{24}$$

at the boundary vibration frequency at $\beta=1$

$$\Delta_i=(-1)^i\frac{F_0e^{j(\omega t+\varphi_0)}\left\{4M\,(n-i+1)-m\left[2(n-i)+1\right]\right\}}{4s\left[M\,(2n+1)-mn\right]} \tag{25}$$

where $\beta=\sqrt{\omega^2 m/4s}$; $\tau=\arcsin\beta$; $\gamma_+=\beta+\sqrt{1-\beta^2}$; $\gamma_-=\beta-\sqrt{1-\beta^2}$; $i=1,\,2,\,3,\,\dots,\,n+1$.

The electrical filter circuit corresponding to the Fig. 4a is shown in Fig. 4b. In accord with the relationships DEMA (8) and (23 – (25), the oscillations in this circuit will obey the following regularities:

at the filter pass band, $\beta_{el}<1$

$$\dot U_i=-\frac{i_0e^{j(\omega t+\varphi_0)}\sqrt{-\dot Z_1\dot Z_2}\left\{\sqrt{-\dot Z_1\dot Z_2}\sin\left[2(n-i)+2\right]\tau+\dot Z_{load}\cos\left[2(n-i)+1\right]\tau\right\}}{\left\{\sqrt{-\dot Z_1\dot Z_2}\cos\left[2n+1\right]\tau-\dot Z_{load}\sin 2n\tau\right\}} \tag{26}$$

at the stop band, $\beta_{el}>1$

$$\dot U_i=(-1)^{i+1}\frac{i_0e^{j(\omega t+\varphi_0)}\sqrt{-\dot Z_1\dot Z_2}\left[\sqrt{-\dot Z_1\dot Z_2}\left(\gamma_{el+}^{2(n-i+1)}-\gamma_{el-}^{2(n-i+1)}\right)+\dot Z_{load}\left(\gamma_{el+}^{2(n-i)+1}-\gamma_{el+}^{2(n-i)+1}\right)\right]}{\left[\sqrt{-\dot Z_1\dot Z_2}\left(\gamma_{el+}^{2n+1}-\gamma_{el-}^{2n+1}\right)+\dot Z_{load}\left(\gamma_{el+}^{2n}-\gamma_{el+}^{2n}\right)\right]} \tag{27}$$

and at the cutoff frequency, $\beta_{el}=1$

$$\dot U_i=(-1)^{i+1}\frac{i_0e^{j(\omega t+\varphi_0)}\sqrt{-\dot Z_1\dot Z_2}\left\{4(n-i+1)\dot Z_2+\left[2(n-i)+1\right]\dot Z_{load}\right\}}{2s\left[(2n+1)\dot Z_2-n\dot Z_{load}\right]} \tag{28}$$

In the case $\dot Z_{load}=\infty$ corresponding to $M=0$, (26) – (28) transform into (9) – (11). At $\dot Z_{load}=0$ ($M=\infty$) the solutions (26) – (28) transform into those similar (16) –(18) at the condition that the output

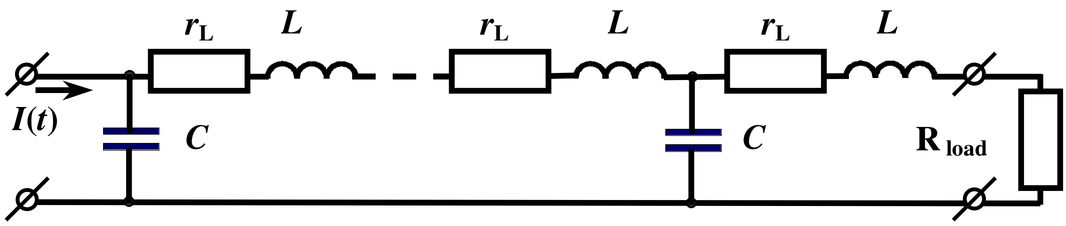

Fig. 5. The schematic diagram of the ***RLC*** ladder filter loaded by an active resistance

of the filter $(n+1)$th node is shorted. At $\dot{Z}_{load} = \dot{Z}_2$ the solutions (26) – (28) also transform to those like (9) – (11) at the conditions of an unloaded $(n+1)$th node of the ladder filter. And only at the condition

$$\dot{Z}_{load} = -j\sqrt{-\dot{Z}_1\dot{Z}_2}e^{-j\tau} \text{ or } \dot{Z}_{load} = j\sqrt{-\dot{Z}_1\dot{Z}_2}e^{j\tau}, \tag{29}$$

unrealisable in frames of the existing circuitry, the conditions for a pure progressive wave along-the-circuit propagation take place at all the pass band, and (26) – (28) take the form generalising the solutions for semi-finite ladder filters that was presented in [6]. In particular, for the negative delay phase these solutions take the following form:

$$\begin{cases} \dot{U}_i = -ji_0\sqrt{-\dot{Z}_1\dot{Z}_2}e^{j[\omega t+\varphi_0-(2i-1)\tau_{el}]};\ \beta_{el} < 1 \\ \dot{U}_i = (-1)^{i+1} ji_0\sqrt{-\dot{Z}_1\dot{Z}_2}\gamma_{el-}^{(2i-1)}e^{j(\omega t+\varphi_0)};\beta_{el} > 1 \\ \dot{U}_i = (-1)^{i+1} ji_0\sqrt{-\dot{Z}_1\dot{Z}_2}e^{j(\omega t+\varphi_0)};\ \beta_{el} = 1 \qquad i = 1,\ 2,\ ...,\ (n+1) \end{cases} \tag{30}$$

In all other cases, a complex superposition of the progressive and standing waves will take place in the filter. Or rather, the conventional formulation of such type of superposition does not reflect enough completely the essence of processes, since the expression (26) more corresponds to the complex superposition of two standing waves. However, further we will show on a specific example that the signal phase at the filter calculated nodes ($i = 1,\ 2,\ ...\ ,\ (n+1)$) generally vanishes only in a countable number of points of the amplitude-frequency characteristic, evidencing the standing wave arising in the filter. Out of these points, dependently on the frequency and number of the studied node of the filter, the phase may be as delaying as advancing with the retaining resonance peaks of the signal amplitude.

Another feature of the presented solutions reveals at the complex value of β_{el}, i.e., in case when the ladder filter cannot be presented as an ideal filter of the low or high frequencies. With it the relation between β_{el} and the unity losses its sense, and in the filter only the regime described by (26) can be realised, while (26) becomes true for all the range from zero to infinity. None the less, as the experience of mechanical elastic lines calculation shows and as we will show further for electrical filters, the regularity (26) at complex β_{el} completely describes the processes both at the pass and stop bands of the filter. Only at $\text{Im}\,\beta_{el} = 0$ the expression (26) losses its sense out of the pass band, and the solution takes the form (26) – (28).

To demonstrate more visually the described features of the solutions, determine the input resistance of a ladder r_LLC filter shown in Fig. 5. We choose this circuit because of a few reasons. It is quite simple, lest to cram the investigation with the additional factors. On the other hand, such circuits are often used for signal delay artificial lines. And by the conventional concept, the matched load of the low-frequency filters must be active, which makes the analysis more associative. At the same time, the changes introduced to the circuit comparing with ideal *LC* filters are sufficient to reveal the described effects, and the circuit itself cannot be calculated directly by the two-port method, because it has the mismatched input and output.

Actually, for this circuit the impedances $\dot{Z}_1$ and $\dot{Z}_2$ take the form

$$\dot{Z}_1 = r_L + j\omega L; \quad \dot{Z}_2 = 1/\, j\omega C \tag{31}$$

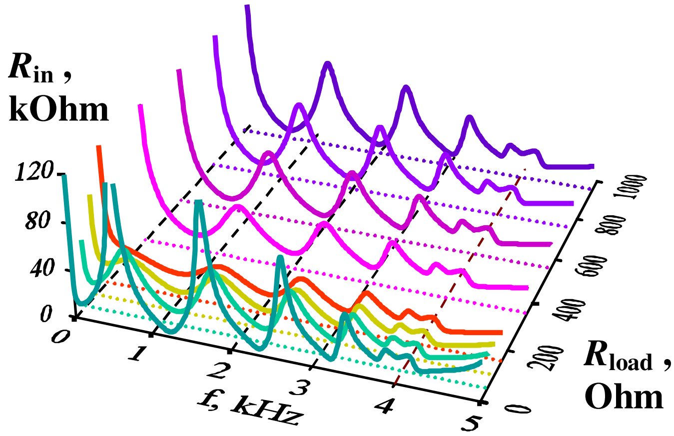

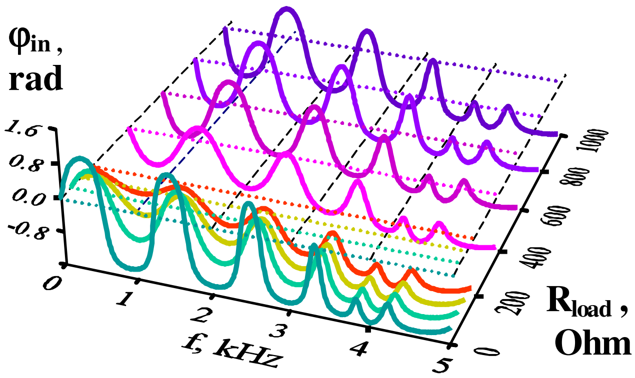

Fig. 6. The calculated amplitude-frequency (a) and phase-frequency (b) characteristics of the input resistance $\boldsymbol{R_{in}}$ at different active load values $\boldsymbol{R_{load}}$ and constant input current value $\boldsymbol{I(t)}$ with respect to frequency. The investigated filter parameters: L = 12,6 mH; C = 0,5 mF; R_0 = 159,15 ohm; r_L = 10 Ohm; R_1 = 20 kOhm; R_2 = 33 kOhm; R_{load} = 0, 51, 102, 158, 358, 558, 758, 958 Ohm.

In accord with (9) – (11) and (31), the parameter β_{el} becomes a complex value

$$\beta_{el} = \frac{1}{2}\sqrt{\omega^2 LC - j\omega r_L C} = \frac{1}{2}\sqrt{\rho_\beta}\, e^{-j\varphi_\beta/2}, \tag{32}$$

where $\varphi_\beta = \arcsin(\omega r_L C/\rho_\beta)$, $\rho_\beta = \omega C\sqrt{\omega^2 L^2 + r_L^2}$. With it the parameter τ_{el} becomes the complex function of the frequency and circuit parameters, and the relationship between β_{el} and the unity losses its sense. As we said before, in this case (26) is true for all the range, while (27) and (28) loss their sense too. As we see, to reveal the complex pattern of β_{el}, we need not consider complex ladder filters. It is sufficient for it even in LC filters simply to note the real parameters of the elements, such as inductive parasitic resistance, capacitive parasitic resistance, and sometimes the connecting wire resistance. In all these cases we can apply (26) to all the range. And if the parasitic parameters influence is small, this expression will simply describe the regularity, practically identical to (26) – (28) for an ideal filter. At the same time, a clear differentiation of the pass and stop bands and the calculation simplicity are the merits of the system (26) – (28). For the case of complex β_{el} the calculation essentially complicates when real and imaginary parts of (26) separating, and it is difficult to determine the boundary frequency from the solution itself. In the studied specific problem, the input resistance R_{in} can be easy determined from (26):

$$R_{in} = \frac{\dot{U}_1}{I(t)} = -\frac{\eta\left(\eta \sin 2n\tau_{el} + R_{load}\cos(2n-1)\tau_{el}\right)}{\left(\eta\cos(2n+1)\tau_{el} - R_{load}\sin 2n\tau_{el}\right)} \tag{33}$$

where

$$\eta = \sqrt{-\dot{Z}_1\dot{Z}_2} = \sqrt{j\frac{r_L}{\omega C} - \frac{L}{C}} = \sqrt[4]{\frac{r_L^2}{\omega^2 C^2} + \frac{L^2}{C^2}}\; e^{j\left(\frac{\pi}{4}+\frac{\varphi_\eta}{2}\right)}$$

The typical form of the amplitude (a) and phase (b) of the input resistance with respect to frequency ω and load R_{load} is shown in Fig. 6. First of all we see that for the finite ladder filter the amplitude and phase of the input resistance has the resonance form. And the number of peaks is different at $R_{load} < R_0$ and $R_{load} > R_0$. It is caused by the fact that at small R_{load} the filter behaves as the shorted and consisting of $n+1$ calculation nodes, and at large R_{load} the input resistance corresponds to an unloaded filter consisting

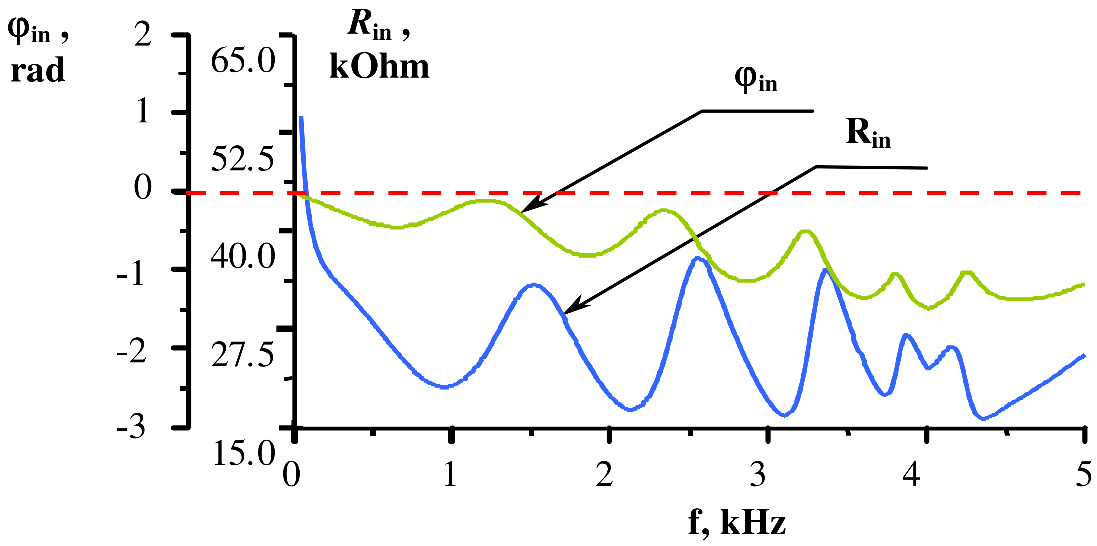

Fig. 7. The combined plot of the amplitude-frequency and phase-frequency characteristics of the low-frequency ***RLC*** filter consisting of 5 sections and loaded onto the impedance R_0 = 159,15 Ohm.

of n nodes, which is in full correspondence with the above analysis of the solutions (26) – (28) transformation. With the growing load resistance the phase characteristic also transforms, up to changing the sign at definite bands. This transformation of the amplitude and phase characteristics takes place at a quite narrow range, where the values R_{load} are lower or higher than the impedance R_0 that is equal in this calculation to 158,15 Ohm (the plots at this value of the load resistance are shown in red). One can see that with growing R_{load} from zero to R_0, the peak amplitudes fall, and at $R_{load} = R_0$ reach some minimum. With the following increase of the impedance, the resonance peaks at the low and medium bands displace, the first resonance peak vanishes, and already at $R_{load} \approx 600\,\text{Ohm}$ (for the present circuit parameters) the resonance frequencies location stabilises at the new number of the resonance frequencies. Further only the resonance peaks themselves grow. And this last concerns to a large extent to the amplitude-frequency characteristic. The resonance peaks on the phase-frequency characteristic reach fast the saturation amplitude not exceeding $\pi/2$ for the first peak.

Especially note that at the band near the cutoff frequency the transformations are practically absent. It evidences that it is basically impossible to choose the load resistance so that it provided the plate of the amplitude-frequency characteristic at the filter pass band.

Furthermore, we see from the plots that at the pass band the input resistance phase not only is not zero, which would correspond to the real value R_{in}, but it multiply alternates the sign, taking by turns the inductive or capacitive pattern. With it the clear correlation between the amplitude and phase resonance peaks is absent too. To demonstrate it, we show in Fig. 7 a combined plot of the input resistance amplitude and phase for the case $R_{load} = R_0$. This evidences that in ladder filters one can obtain plate neither an amplitude-frequency nor a phase-frequency characteristic of the filter input resistance, at no active load value. Even if at some load resistance a definite smoothing of the characteristics were possible in the pass band low-frequency domain, near the cutoff frequency the regularities have resonance pattern and practically do not transform with the load resistance variation.

The same we see in case of complex loading. As an example, in Fig. 8 we show the amplitude and phase-frequency characteristics over the $r_L LC$ filter investigated before, when it is loaded by the sequentially connected active $R_{load} = R_0$ resistance and capacitive C_{load} impedance. In the plots we see alike transformations of the regularities with the C_{load} variation, only the resonance peaks amplitude monotonously grows with the capacitance falling. Now some value of capacitance approximately equal to 1 mcF at the chosen circuit parameters serves the transition border. In the region of this capacitive load, in the

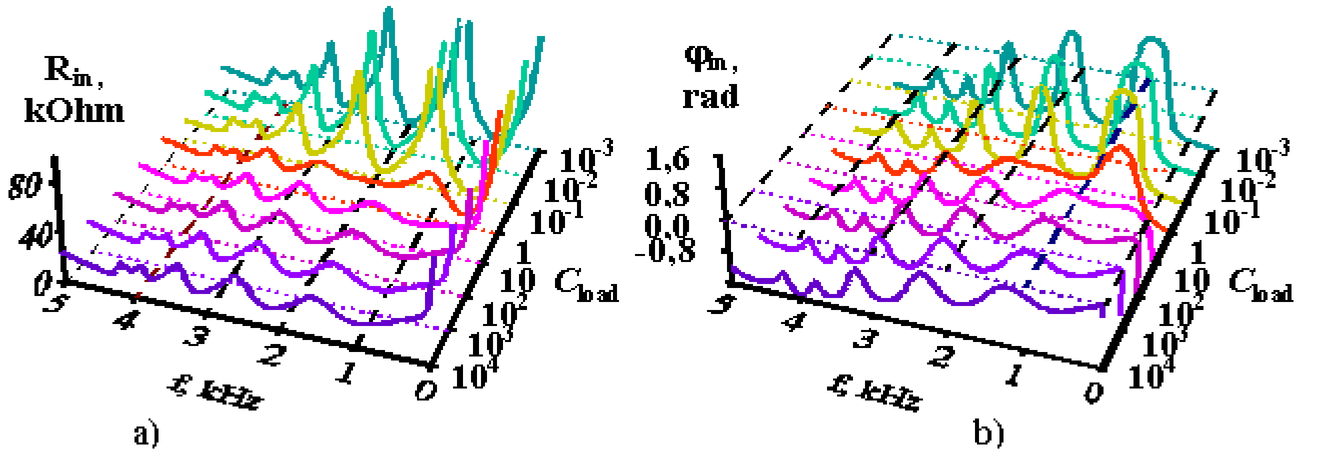

Fig. 8. The calculated amplitude-frequency (a) and phase-frequency (b) characteristics of the input resistance R_{in} at different load capacitance values C_{load} and constant value of the input current amplitude $I(t)$ with respect to frequency. The investigated filter parameters: L = 12,6 mH; C = 0,5 mF; R_0 = 159,15 Ohm; r_L = 10 Ohm; R_1 = 20 kOhm; R_2 = 33 kOhm; R_{load} = 158 Ohm.

low-frequency domain of the pass band, the curves displace, and the new resonance peak merges with the first peak of the previous characteristic. Thus, with the falling load capacitance, the quantity of resonance peaks does not change, and even their location along the frequency axis retains out of the transition domain. And again, all described transformations occur in the low- and middle-frequency domains of the pass band, with practically flat pattern at the cutoff frequency.

To check up the obtained calculation regularities, we have carried out the experiment whose circuit is shown in Fig. 9. Its principal aim was to investigate the amplitude-frequency and phase-frequency characteristics of the input resistance at the ladder filter pass band with the constant input current amplitude $I(t)$. The introduced condition of the input current (not voltage) constancy was caused, on one hand, by the dependence of solutions (26) on the input current amplitude. And on the other hand, when experimenting, it is convenient to compare voltages, not currents. Moreover, the phase characteristics measurement between the voltages excludes a number of essential systematic errors.

Basing on the above arguments, we worked out the experimental scheme. One can see from Fig. 9 that the phase of the filter input resistance was measured as the difference between the voltage phases at the source output and at the ladder filter input. For it between the source output and filter input we inserted quite large resistor R_1 stabilising the phase of the source output voltage. The second task of this resistor was to bring the experimental conditions at the filter input nearer to the calculated conditions, according to which the filter input was loaded (see Fig. 5).

The pattern of input resistance variation with frequency was investigated by the voltage variation at the filter input being equivalent to the constant input current amplitude. The experimental data were picked off the screen of oscillograph having a large input resistance (>1 MOhm), small input capacitance ($\sim 40 \mu\mu F$) and the resolving ability in frequency more than 10 MHz. To reduce the measurement error, we used the one-ray oscillograph with the measurement channels switching at its input (the switch SA1). To reduce the standard error of the oscillograph (about 5%) when the phase characteristics measuring, we used the maximal sweep with the external synchronisation, and when investigating the amplitude characteristics – the maximal amplification of the signal and measuring the oscillation swing.

The results – the amplitude-frequency (a) and phase-frequency (b) characteristics – are presented in Fig. 10. This first has the form of regularity of the acting voltage amplitude at the filter input with respect to frequency and input resistance. And the second has the form of displacement phase in radians, also with respect to frequency and input resistance. Comparing them with the calculation diagrams in Fig. 6, we see a full accord of the patterns accurate to the experimental error. The only difference is in the amplitude values of the resonance peaks when comparing the experimental and calculation data. The

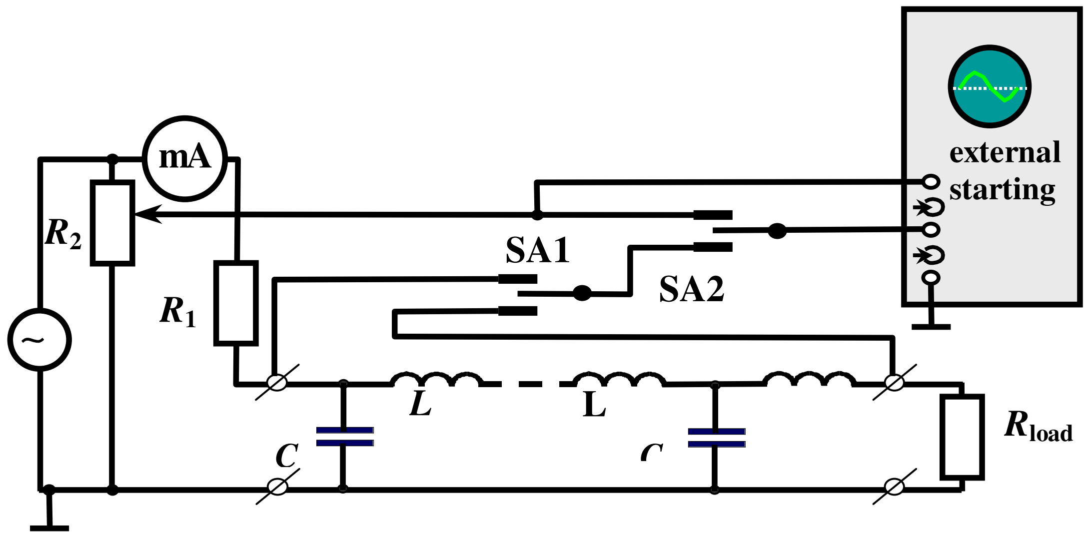

Fig. 9. The schematic diagram of the experimental setup to measure the amplitude-frequency and phase-frequency characteristics of the ***LC***-type ladder filter. The setup parameters: L = 12,6 mH; C = 0,5 mF; R_0 = 159,15 Ohm; r_L = 10 Ohm; R_1 = 20 kOhm; R_2 = 33 kOhm; R_{load} = 0, 51, 102, 158, 358, 558, 758, 958 Ohm.

calculated amplitude is some higher. This is caused by the finiteness of resistance R_1. Its value is well more than the filter impedance R_0 and is quite large to ensure a good accord of the phase characteristics, but is not quite sufficient, the amplitude characteristics to be in full accord with the calculation circuit. Because, as one can determine by the data in Fig. 6, it is comparable with the maximal value of the input resistance amplitude in the resonance peaks domain. Basically, the presented method allows getting over this disparity too. In this order we should complicate a little the initial mechanical prototype model and consider an elastic line having heterogeneities not only at its output but also at the input. But since our

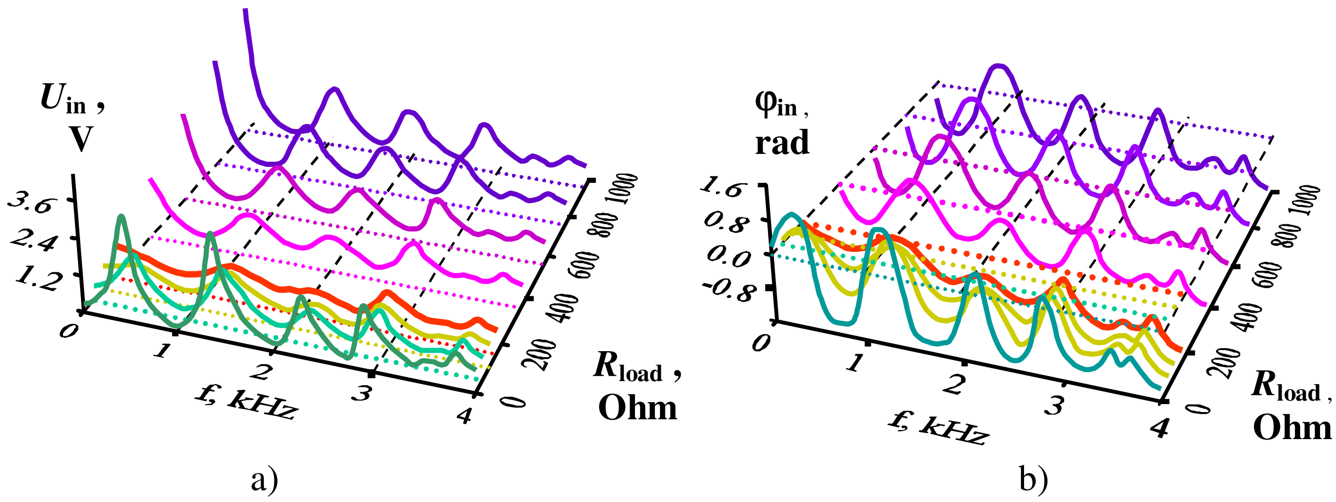

Fig. 10. The experimental amplitude-frequency (a) and phase-frequency (b) characteristics of the input resistance $\boldsymbol{R_{in}}$ at different active load values $\boldsymbol{R_{load}}$ and constant input current value $\boldsymbol{I(t)}$ with respect to frequency. The investigated filter parameters: L = 12,6 mH; C = 0,5 mF; R_0 = 159,15 ohm; r_L = 10 Ohm; R_1 = 20 kOhm; R_2 = 33 kOhm; R_{load} = 0, 51, 102, 158, 358, 558, 758, 958 Ohm.

main aim here is to investigate just the resistance load influence on the vibration pattern, such refinement is out of frames of this paper. While within these frames we can surely state that the presented coincidence of the calculated and experimental results demonstrates quite conclusively that ladder filters cannot be modelled by a simple assemblage of elementary two-ports in general case. Their amplitude and phase characteristics have the complex resonance form well described by the combined method based on the exact analytical solutions for mechanical elastic lines as the analogue and the dynamical electromechanical analogy DEMA. With it the ladder filter structure can be much complicated, if necessary, even in frames of the problem solved here, since one can think under the impedances $\dot{Z}_1$ and $\dot{Z}_2$ any complex impedance, in that number the input impedance of the filter branches. In all these cases the DEMA relationship retain true, because they take into account the similarity of just the dynamical processes in mechanical lines and ladder filters.

5. Conclusions

We have analysed the solutions for finite ladder filters obtained on the basis of the exact analytical solutions for corresponding mechanical elastic lumped lines and original methods of the dynamical electromechanical analogy DEMA. We have ascertained that finite ladder filters cannot be considered as a simple assemblage of the elementary two-ports, summing their delay phases and multiplying the transmission coefficients. As a result of multiple reflections from the ends in finite filters, in the amplitude-frequency and phase-frequency characteristics of the filter there arise the resonance phenomena effecting on the transmission coefficient and total delay phase. It reflects also on the filter input resistance characteristic inequal to the impedance and not active at the pass band in general case. The progressive wave can arise in the filter only in case of reciprocal trigonometric dependence of the load phase on frequency, which is unrealisable with the currently existing circuitry.

By way of $r_L LC$ filter as an example we have proved theoretically and corroborated experimentally that with the filter active load variation the main transformations of the amplitude-frequency and phase-frequency characteristics take place in the low and middle domains of the pass band. With the growing resistance of the load up to the value close to that characteristical, the resonance peaks amplitude falls. With the further increase of resistance, the first peak frequency vanishes and the number of peaks diminishes by an unity. With it the peak amplitude gradually grows again. In case of the active-capacitive load, with the diminishing capacity the resonance peaks amplitudes gradually grow, but the number of peaks does not change, only a newly arisen peak merges with the first resonance peak of the filter.

The results presented here can be extended to more complicated ladder filters.

References

1. Bonch-Bruevich, A. M. *Radio electronics in experimental physics*. Nauka, Moscow, 1966, 768 pp. (Russian)
2. Zernov, N. Z., and Karpov, V. G. *Theory of radio engineering circuits*. Energy, Moscow – Leningrad, 1965, 886 pp. (Russian)
3. Gurevich, I. V. *Computational foundations of radio engineering networks (Linear networks under harmonic action)*. Svyaz’, Moscow, 1975, 366 pp. (Russian)
4. Kugushev, A. M., and Golubeva, N. S. *Foundations of radio rlectronics*. Energia, Moscow, 1969, 880 pp. (Russian)
5. A.S. Hu, F.W. Lam and C. Lin. Recursive formulas of a multiple-sectioned transmission line. *IEEE Transactions on circuits and systems*, CAS-21, 5 (September 1974), pp.640-642
6. S.B.Karavashkin. Refined method of electric long lumped-parameters line calculation on the basis of exact analytical solutions for mechanical elastic lines. *Control of Oscillations and Chaos 2000*. Proceedings of the conference, vol.1, p.154. St.Petersburg, Russia, 2000.
7. Gardner, M. F. and Barns, J. L. *Transients in linear systems with lumped parameters*. Inostrannaya literatura, Moscow, 1961, 570 pp. (Russian; original edition: M. F. Gardner and J. L. Barns. *Tran-*

sients in Linear Systems, vol.1: Lumped-constant systems. John Wiley & Sons Inc., NY, and Chapman & Hall ltd, London, 1942)

8. Karplus, W. J. *Analog simulation solution of the field problems*. Inostrannaya literatura, Moscow, 1962, 488 pp. (Russian; original edition: W.J. Karplus. *Analog Simulation Solution of Field Problems*. McGraw-Hill Book company Inc., New York – Toronto – London, 1958).
9. Atkinson, F. V. *Discrete and continuous boundary problems*. Mir, Moscow, 1968, 750 pp. (Russian; original edition: Atkinson, F. V. *Discrete and Continuous Boundary Problems*. Academic Press, New York – London, 1964)
10. S.B.Karavashkin. Exact analytical solution on infinite one-dimensional elastic lumped-parameters line vibration. *Materials, Technologies, Tools*. The Journal of National Academy of Sciences of Belarus, 4 (1999), 3, pp.15 – 23 (Russian)
11. S.B.Karavashkin. Exact analytical solution on finite one-dimensional elastic lumped-parameters line vibration. *Materials, Technologies, Tools*. The Journal of National Academy of Sciences of Belarus, 4 (1999), 4, pp.5 – 14 (Russian)
12. Gutenmaer, L. I. Introduction to the Russian edition of the book by W. J. Karplus [8].
13. *Physical encyclopaedia*, vol. 5. Sovetskaya Encyclopedia, Moscow, 1966.